

Angular correlations in single-top-quark and Wjj production at next-to-leading order

Zack Sullivan

High Energy Physics Division, Argonne National Laboratory, Argonne, Illinois 60439, USA

(Dated: October 13, 2005)

Abstract

I demonstrate that the correlated angular distributions of final-state particles in both single-top-quark production and the dominant Wjj backgrounds can be reliably predicted. Using these fully-correlated angular distributions, I propose a set of cuts that can improve the single-top-quark discovery significance by 25%, and the signal to background ratio by a factor of 3 with very little theoretical uncertainty. Up to a subtlety in t -channel single-top-quark production, leading-order matrix elements are shown to be sufficient to reproduce the next-to-leading order correlated distributions.

PACS numbers: 14.65.Ha, 12.38.Bx, 13.85.Lg, 13.87.Ce

arXiv:hep-ph/0510224v2 4 Nov 2005

I. INTRODUCTION

The discovery of single-top-quark production is one of the primary goals of run II of the Fermilab Tevatron. In recent years it has become apparent [1, 2, 3, 4] that a modest b -tagging efficiency and larger-than-expected jet energy resolution have promoted Wjj production to the most important background to single-top-quark production. In order to overcome a poor signal to background ratio of $\sim 1/10$ [3, 4], recent theoretical studies [5, 6] have shown that only modest improvements can be made by improving cuts in pseudorapidity or b -jet assignment.

It was demonstrated in Ref. [7] that a spin correlation between the final-state lepton and non- b jet in single-top-quark production might provide an effective discriminate against the Wjj backgrounds. Both the CDF and D0 Collaborations have used this correlation at some level to improve their analyses. Nevertheless, the theoretical basis for this has only been confirmed at leading order (LO). Hence, several questions arise:

1. Do the strong spin correlations that appear at LO in single-top-quark production survive higher-order radiation, and leave distinctive angular correlations in the final-state particles?
2. Is the background really insensitive to the angular distributions that typify the signal? If so, does this survive complex cuts on the data?
3. These correlated angular distributions are properly defined in the reconstructed rest frame of the top quark. How much of these correlations is an artifact of that choice of frame?
4. Do these correlations lead to better discriminates between the signal and backgrounds? Are there other particle correlations that have been missed?

In this paper, I address all of these issues, and demonstrate the need to account for the fully-correlated angular distributions. First I clarify exactly how the Mahlon-Parke [8] spin-basis works, and why it does so surprisingly well for both s - and t -channel single-top-quark production. In Sec. II, I describe the exact effects of higher orders on the angular correlations for both single-top-quark production and Wjj backgrounds. Angular correlations can be induced in the Wjj background that make it look like the signal. Avoiding these problems

requires that cuts be made on the fully-correlated (multidimensional) angular distributions, as discussed in Sec. III. I present some evidence that an invariant-mass distribution may be a useful discriminate, and provide a representative set of cuts that improve the significance by at least 25%, and the signal to background ratio by a factor of 3 with very little theoretical uncertainty.

Before describing higher-order effects on angular distributions, we must first understand why we expect there to be strong angular correlations. In Ref. [8], an optimal basis was introduced to measure the spin-induced correlations in single-top-quark production. The matrix elements for both s -channel and t -channel single-top-quark production (seen in Fig. 1) are proportional to

$$[p_d \cdot (p_t - m_t s_t)][p_e \cdot (p_t - m_t s_t)], \quad (1)$$

where p_d and p_e are the four-momenta of the down-type quark and charged lepton in the event, p_t and m_t are the top-quark four-momentum and mass, and s_t is top-quark spin four-vector. In the top-quark rest frame $p_t = m_t(1, 0, 0, 0)$, and $s_t = (0, \hat{s})$.

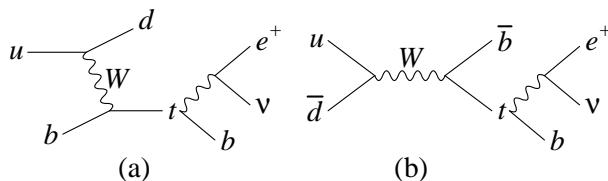


FIG. 1: Representative leading-order Feynman diagrams for (a) t -channel, and (b) s -channel production of a single top quark.

When looking at s -channel production, the direction of the down-type quark provides a convenient axis to project the top-quark spin, i.e., choose $\hat{s} = \hat{d}$ as in Fig. 2. Then the matrix element reduces to $E_d E_e m_t^2 (1 + \cos \theta_{e+\bar{d}}^t)$. Since roughly 98% of the events at the Fermilab Tevatron are produced by pulling a \bar{d} from the incoming antiproton, measuring $\cos \theta_{e+\bar{p}}^t$ provides the best possible measure of the spin correlation.

Angular correlations in t -channel single-top-quark production are more complicated. The d quark ends up in the highest- E_t non- b -tagged jet j_1 approximately 3/4 of the time. Hence, it makes sense to measure $\cos \theta_{e+j_1}^t$. The rest of the time a \bar{d} -quark is in the initial state, and hence a perfect correlation exists with the incoming hadron (mostly the antiproton at the Tevatron). Nevertheless, there is still a strong correlation in these events with the

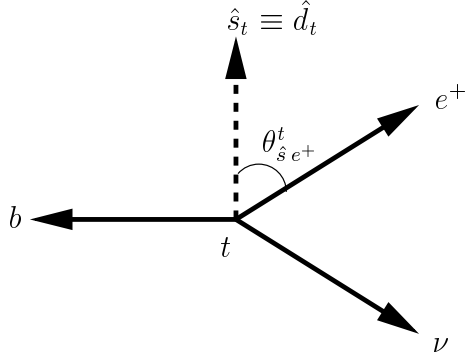


FIG. 2: Decay products of the top quark, and the angle $\theta_{\hat{s}_t e^+}^t$ between the charged lepton e^+ and the spin \hat{s}_t of the top quark in the top-quark rest frame. It is convenient to choose the spin to be projected in the direction of the down-type quark d in the event.

direction of j_1 . In this case, if we project the spin in the direction of the final-state jet (which comes from a \bar{u}), the matrix element is proportional to $(1 + \cos \theta_{d j_1}^t \cos \theta_{e^+ j_1}^t)$. The dilution factor $\cos \theta_{d j_1}^t = 1 - Q^2/(E_d^t E_{j_1}^t)$ has a typical value of 0.86 with no cuts, and 95% of the time is more than 0.5. The dilution is a small effect in a small fraction of the events. Hence, $\cos \theta_{e^+ j_1}^t$ is an excellent quantity to measure. The saving grace here was a kinematic correlation induced by the t -channel exchange of the W boson. We will return to the effects of these “kinematically-induced correlations” in single-top-quark and Wjj production in each of the Sections below.

II. ANGULAR CORRELATIONS AT LO AND NLO

Given the strength of the spin correlations in single-top-quark production, it is natural to want to use these as a discriminate between the signal and backgrounds. In order to be effective, however, we must know that these correlations will actually appear in the data. Before reaching the issue of detector effects, we must first address whether these correlations are an artifact of the leading-order calculations that found them, or are real. We begin with the dominant t -channel production cross section.

There are only three ways that QCD radiation at next-to-leading order can degrade the measured angle between the lepton and jet j_1 in t -channel production. The first is radiation off of the top quark before it decays. This can cause a spin flip, but is suppressed by the top quark mass. The second way to dilute the correlation is for the down-type quark to

radiate, and thereby change the measured angle. This is suppressed for typical jets because most radiation is fairly soft and collinear, and is reabsorbed into the final measured jet. Only very energetic wide-angle jets are relevant. The most significant dilution of the spin correlation should therefore come from misidentifying the jet that includes the down-type quark. From this point of view, the effect of next-to-leading order (NLO) radiation is to provide additional jets to misidentify.

The efficiency of $\cos\theta_{ej_1}^t$ as a discriminate for the single-top-quark signal, will ultimately be based upon experimental precision. Nevertheless, we can calculate whether there is an underlying limit based on the rate of misidentification of the direction of the down-type quark in the event. For all calculations in this paper I use MCFM 4.1 [9] (with some corrections¹ to the matrix element for t -channel single-top-quark production based on the NLO code ZTOP [10]). MCFM contains NLO corrections to top-quark decay, as well as full spin correlations for final-state leptons and jets. Figures are presented for t (not \bar{t}) production only at run II of the Fermilab Tevatron, a 1.96 TeV $p\bar{p}$ collider, but the underlying principles apply equally well to the CERN Large Hadron Collider (LHC). CTEQ6L1 and CTEQ6M [11, 12] parton distributions are used for LO and NLO distributions, respectively. The top-quark mass is taken to be 175 GeV.

Acceptance cuts for inclusive $W + 2$ -jet distributions are based on Ref. [3] and listed in Table I. The top quark is reconstructed using the “ b -jet” (chosen randomly if there are an even number of candidates in the final state) and a reconstructed W boson of mass 80.4 GeV. The W boson is reconstructed using an isolated charged lepton and missing transverse energy \cancel{E}_T , where the neutrino solution with the smallest absolute pseudorapidity is chosen. Other neutrino solutions were tested, but found to give worse fits to the top-quark mass. A loose cut on the top-quark mass $M_{be\cancel{E}_T}$ has little effect on the shapes of the distributions presented, but does change the normalization of the backgrounds.

Let us compare t -channel production at LO and NLO. In Fig. 3 we see the differential cross section as a function of $\cos\theta_{ej_1}^t$ at LO. For the cuts in Table I, approximately 4.5% of the events come from a \bar{d} , \bar{s} , or \bar{b} quark in the initial state. The correct direction to project into for these events is the proton direction, since most \bar{d} come from the antiproton. All of the other events (except the small sea-quark contribution) should be in the direction

¹ These have been provided to, and confirmed with, the authors of MCFM.

TABLE I: Acceptance cuts applied to E_T -ordered jets and leptons in the Wjj final state. Require one charged lepton (denoted e throughout), missing transverse energy \cancel{E}_T , and at least two jets. At least one jet must pass the b acceptance (two b jets for s -channel single-top-quark production).

$E_{Tj} > 15 \text{ GeV}, \eta_j < 2.8, \Delta R_{kT} < 0.54 (\approx \Delta R_{\text{cone}} < 0.4)$
$E_{Tb} > 25 \text{ GeV}, \eta_b < 1.4$
$E_{Te} > 15 \text{ GeV}, \eta_e < 1.4, \Delta R_{ej} > 0.4$
$\cancel{E}_T > 15 \text{ GeV}$
$140 < M_{be\cancel{E}_T} < 210$

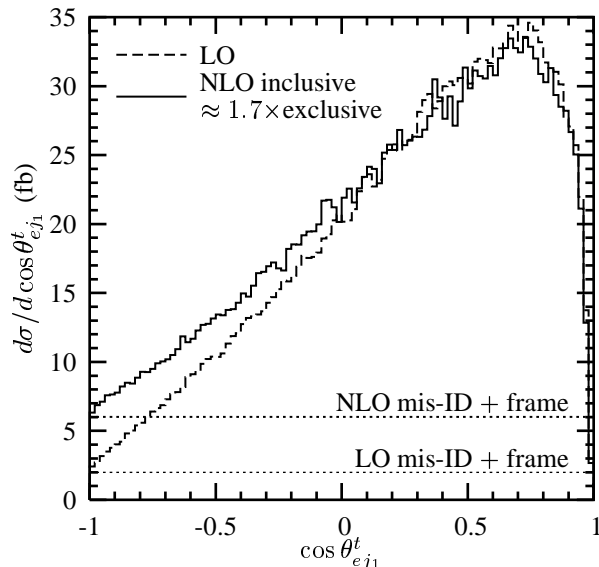


FIG. 3: Cosine of angle ($\cos \theta_{e_{j_1}^t}$) between the charged lepton and highest- E_T light-quark jet in the top-quark rest frame of t -channel single-top-quark production at LO and NLO. The lepton isolation cut suppresses events at large $\cos \theta_{e_{j_1}^t}$. A nearly angle-independent underlying contribution comes from misidentification of which jet contains the down-type quark.

of the highest- E_T jet that did not come from the top-quark decay. So we expect to see a 100% correlation on top of an uncorrelated² “background” of about 4.5%. The dip near

² There is a kinematic anti-correlation between the direction of the proton and the jet containing the \bar{u} or \bar{c} that produces a slight tilt to the background.

$\cos \theta_{ej_1}^t = 1$ is due to the lepton isolation cut.

When we place cuts at LO, the forward jets and leptons are excluded. Therefore, an additional dilution factor of 0.95 is added to the case where the the down-type quark was in the initial state. In Fig. 3 we are reconstructing the top-quark mass by fitting the missing transverse energy \cancel{E}_T to the W -boson mass. This adds a dilution factor of 0.95 to all production modes. The final cross section is then

$$\frac{d\sigma}{d \cos \theta_{ej_1}^t} \approx 21[0.75(1 + 0.95 \cos \theta_{ej_1}^t) + 0.25(1 + 0.95 \times 0.95 \times 0.86 \cos \theta_{ej_1}^t)] \text{ fb}. \quad (2)$$

At NLO the dilution factor from frame reconstruction is slightly worse at 0.9, but the main difference is that there are more jets to misidentify as containing the down-type quark. It was demonstrated in Refs. [7, 10] that a sizable fraction of the leading jets j_1 are actually from wide-angle emission of initial-state \bar{b} jets. For the cuts of Table I, about 8.3% of the events contain a \bar{b} quark. This particle is completely uncorrelated with the direction of the charged lepton. If we add these two effects, we find the correct uncorrelated “background” underneath the signal. The conclusion to be drawn is that the spin correlations are robust when higher-order radiation is included, but confusion in picking the correct correlated jet will slightly dilute the signal in a completely calculable way.

We can appreciate the stability of the spin correlations at NLO by comparing the correlation in the top-quark rest frame to the laboratory frame. We see in Fig. 4 that the lab frame is only slightly worse for observing the correlation. This is due to the fact the top-quark is typically nonrelativistic, and so there is not much of a boost in switching frames. If the top quark momentum were comparable to its mass, the cosine of the angle in the lab frame $\cos \theta_{ej_1}^l$ would be flat. This leads to the fortunate accident that the angular correlation in t -channel production is not very sensitive to how well the top-quark rest-frame is reconstructed.

In s -channel production, the direction of the charged lepton and the antiproton are well measured. The limiting factor in utilizing $\cos \theta_{e\bar{p}}^t$ is how well the top-quark rest-frame is reconstructed. Since the neutrino coming from top-quark decay is not observed, it is typically reconstructed from the missing transverse energy and a fit to the W mass. We see in the dashed line of Fig. 5 the already sizable effect of this approximate fit on the distribution of $\cos \theta_{e\bar{p}}^t$. s -channel production has the additional difficulty that it is typically impossible to tell which of the two b -jets came from the top quark decay. The simplest choice for

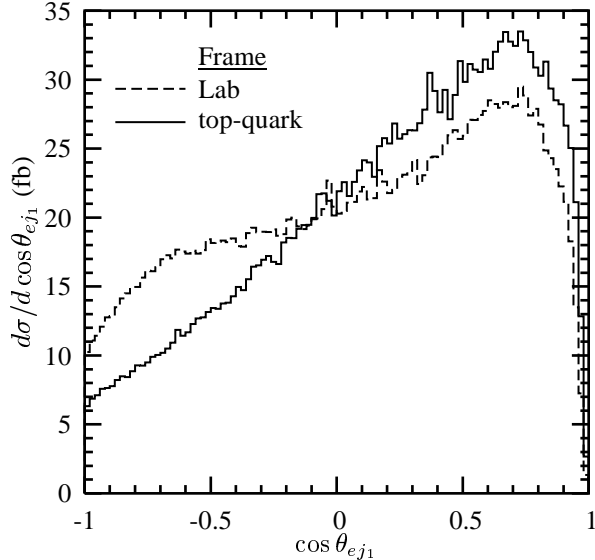


FIG. 4: Cosine of angle ($\cos \theta_{ej_1}$) between the charged lepton and highest- E_T light-quark jet j_1 in the lab frame and top-quark rest frame of single-top-quark production at NLO.

reconstructing the top quark is to randomly choose one of the two b jets. The dotted line in Fig. 5 shows what the measured correlation would look like given this choice. We will investigate in Sec. III whether other choices of assigning the b jet that came from the top quark are useful discriminates from the background. It is apparent, however, that the shape of this distribution is the same at LO and NLO. The only difference is a K -factor of 1.4, which is consistent with the results of Refs. [10, 13].

It was shown in Refs. [7, 14] that the Wjj background at LO is almost flat in the distribution $\cos \theta_{ej_1}^t$. We now wish to test this at NLO. In Fig. 6 the Wjj and $Wb\bar{b}$ backgrounds³ are shown at LO and NLO scaled to match the LO cross section. It appears that LO provides a good description of the shape of the $\cos \theta_{ej_1}^t$ distribution. The shape of the $\cos \theta_{e\bar{p}}^t$ distribution is shown in Fig. 7, and is also well-approximated by LO times a NLO K -factor. Therefore, up to the issues mentioned in t -channel reconstruction, LO matrix elements provide excellent approximations to both the signal and backgrounds for single-top-quark production.

³ Note, the QCD $Wc\bar{c}$ and $Wb\bar{b}$ backgrounds are identical before detector effects are applied.

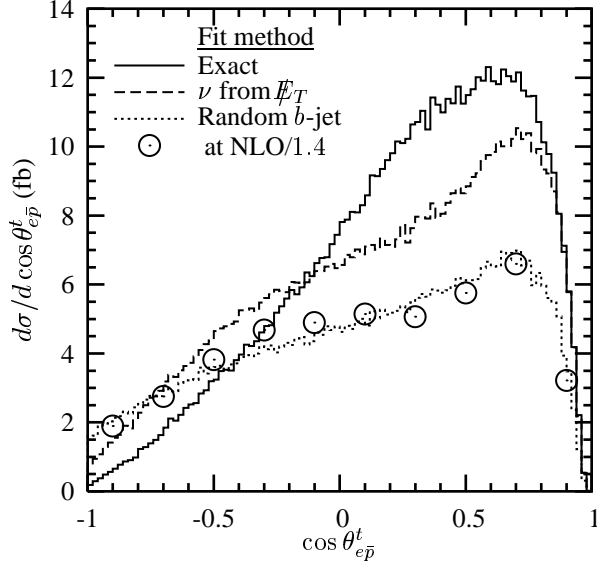


FIG. 5: Cosine of the angle ($\cos \theta_{e\bar{p}}^t$) between the charged lepton and antiproton in the top-quark rest frame of s -channel single-top-quark production at LO at the Fermilab Tevatron (a 1.96 TeV $p\bar{p}$ collider). The solid line corresponds to reconstructing the top-quark frame using the exact neutrino and b -jet from the top-quark decay. The dashed line uses the missing transverse energy and W mass to fit a putative neutrino momentum. The dotted line adds the effect of using a randomly chosen b -jet. The rescaled NLO cross section with a randomly chosen b jet is indicated by open circles.

III. CORRELATED ANGULAR DISTRIBUTIONS

Having established that the angular correlations are stable between LO and NLO, we now turn to whether they are a useful discriminant. The first correlation we examine is between the charged lepton, denoted as e^+ , and the b jet from the top-quark decay. In a top-quark decay the b jet recoils against a real W , which then decays to two leptons. We therefore expect there to be a large angle between e^+ and b . This is borne out in the distributions shown in Fig. 8. Recall that for t -channel production the charged lepton and j_1 have a $1 + \cos \theta_{ej_1}^t$ distribution. We expect, then, that $\cos \theta_{eb}^t < \cos \theta_{ej_1}^t$, as depicted in Fig. 9. This is true roughly 80% of the time for both s -channel and t -channel production. Hence, we might expect we have a better discriminate than b -tagging for t -channel production, and an excellent way to determine which of the two b -jets in s -channel production came from the top-quark decay.

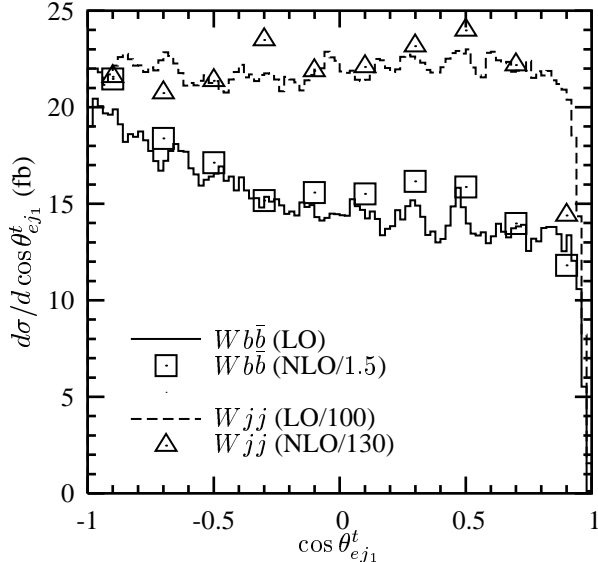


FIG. 6: Cosine of angle ($\cos \theta_{ej_1}^t$) between the charged lepton and highest- E_T light-quark jet j_1 in the M_{Wb} rest frame of $Wb\bar{b}$ (solid), and Wjj (dashed) production at LO, where one of the two highest- E_T jets is randomly tagged as a b -jet, and the other is j_1 . The NLO cross sections are shown scaled to the LO cross sections.

Ignoring b -tagging, let us begin with the two highest- E_T jets in the event. Define the “ b -jet” to be the jet with the largest opening angle in the reconstructed e -jet- \cancel{E}_T rest frame (the putative top-quark rest frame before mass cuts). Up to a normalization factor of 1.3, the $\cos \theta_{e\bar{p}}^t$ for s -channel production now follows the exact result in Fig. 5 when $\cos \theta_{e\bar{p}}^t < -0.2$, and the dashed line from Fig. 5 at larger $\cos \theta_{e\bar{p}}^t$. Hence, this definition effectively removes the b -jet assignment uncertainty in the accepted events. The real question is: what does this do to the Wjj background in general? In Fig. 10 we see that it takes the initially flat Wjj backgrounds, and shapes them to look just like the original t -channel signal! It looks like we’ve taken a step backward, but we will see in Sec. III A that this will be fine.

First, let us understand why the Wjj distribution has the shape it does. This is a generic effect of the cut we have made. On the left side of Fig. 11 we see a function that is completely flat in two variables a and b . If we make the cut $a < b$, and plot the projection of b , we immediately see that we have induced a correlation that was not previously present. The right side of Fig. 11 is closer to the situation we have from Fig. 8, with $a \approx \cos \theta_{eb}^t$ and $b \approx \cos \theta_{ej_1}^t$ for Wjj (or $Wb\bar{b}$). Aside from a small variation, the rough shape is always the same. The reason $\cos \theta_{eb}^t$ is peaked at large angles is that we have shifted the distribution,

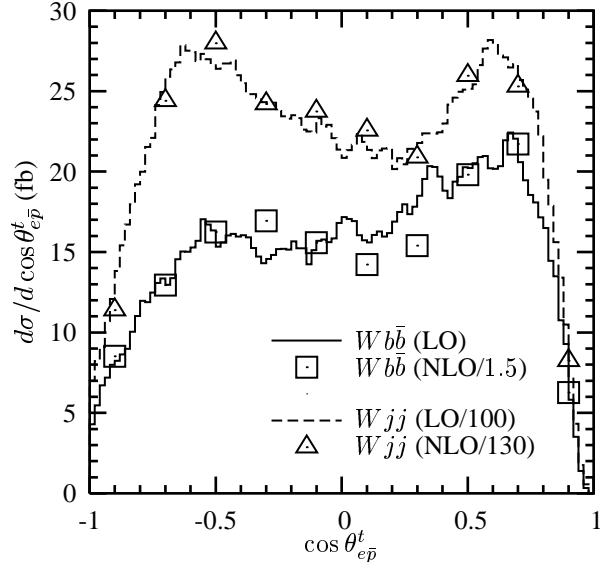


FIG. 7: Cosine of angle ($\cos\theta_{e\bar{p}}^t$) between the charged lepton and antiproton in the M_{Wb} rest frame of $Wb\bar{b}$ (solid), and Wjj (dashed) production at LO, where one of the two highest- E_T jets is randomly tagged as a b -jet. The NLO cross sections are shown scaled to the LO cross sections.

which is symmetric in the lab frame, by boosting the top-quark rest frame defined by the W and b . This should serve as a reminder that any cut on angular distributions will induce some correlation.

Though we may be tempted to ignore this angular cut as a failed trial, we should recognize that there are two common experimental realities that are roughly equivalent to the cut $\cos\theta_{eb}^t < \cos\theta_{ej_1}^t$. First, the efficiency for tagging (or mistagging) a jet generally increases with its transverse energy. Since the highest- E_T jet tends to balance the W boson, its angle with the lepton will on average be larger than for the non-tagged jet. The second common occurrence is the use of a loose top-quark mass reconstruction. Even if the tagging rate was energy-independent, the top quark mass is large enough that only a tagged jet that recoils against the W will pass the cut. Both cases preferentially choose the jet with the largest opening angle to be the tagged jet. Hence, this kinematic correlation will likely always be present at some level in a realistic analysis.

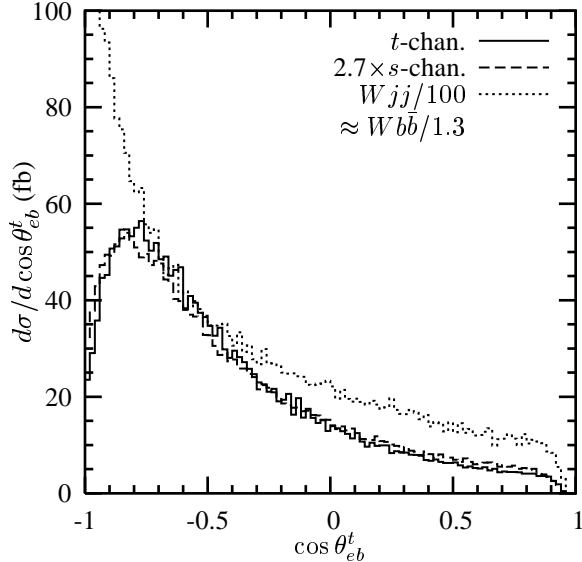


FIG. 8: Cosine of the angle ($\cos \theta_{eb}^t$) between the charged lepton and final-state b quark in the top-quark rest frame. The t -channel and s -channel single-to-quark distributions are the same, since they both involve a real top-quark decay. The Wjj and $Wb\bar{b}$ distributions appear similar to real top-quark decay because of the boost into the top-quark rest frame.

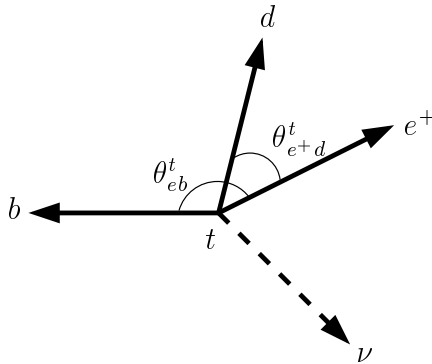


FIG. 9: Particles in the final state of single-top-quark production, in the top-quark rest frame. The angle between the charged lepton e^+ and the b quark is expected to be larger than the angle between e^+ and the down-type quark d .

A. Using full angular correlations

If we wish to make cuts on angular distributions, we must take into account the full angular correlations. There are at least three observed objects in the final state: the charged lepton e (or μ), the b from the top-quark decay, and the other jet j_1 . In Figs. 12–14 we plot

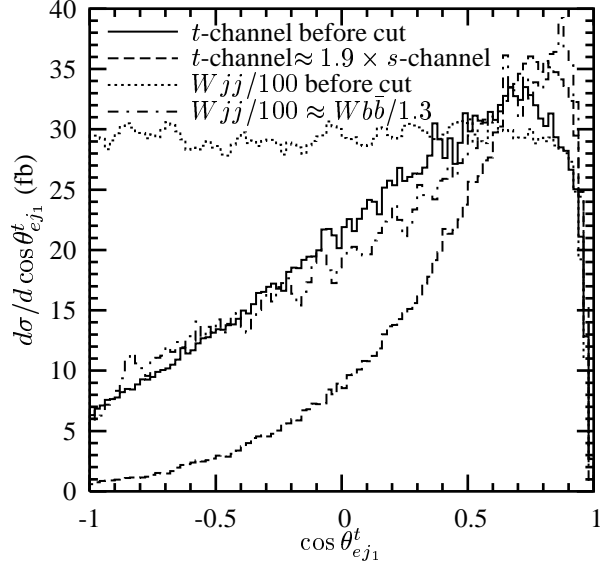


FIG. 10: Cosine of the angle ($\cos \theta_{ej_1}^t$) between the charged lepton and final-state jet j_1 in the top-quark rest frame, before and after the cut $\cos \theta_{eb}^t < \cos \theta_{ej_1}^t$. The t -channel and s -channel single-to-quark distributions are the same after cuts. The Wjj and $Wb\bar{b}$ distributions go from approximately flat to very similar to the t -channel distribution before cuts.

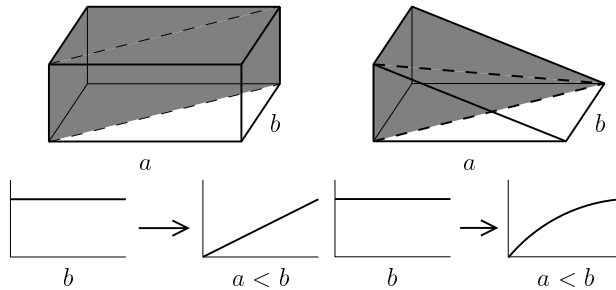


FIG. 11: Effect of the cut $a < b$ on an initially flat distribution b for two cases: (left) completely flat distributions, (right) a falling distribution for a (similar to the actual $\cos \theta_{eb}^t$). The resulting shape for b is an integral over a , and is only modestly sensitive to the detailed shape of a .

the correlated NLO distributions between pairs of these angles in t -channel single-top-quark production. Also shown is the difference (in fb) between the NLO and LO distributions. Except for where new phase space opens up, the difference is less than 3%. The same distributions are shown for s -channel production in Figs. 15–17. The difference between NLO and LO times a K -factor of 1.43 is too small to display.

We can see in Figs. 13 and 16 that the cut we examined in Sec. III was sensible for both

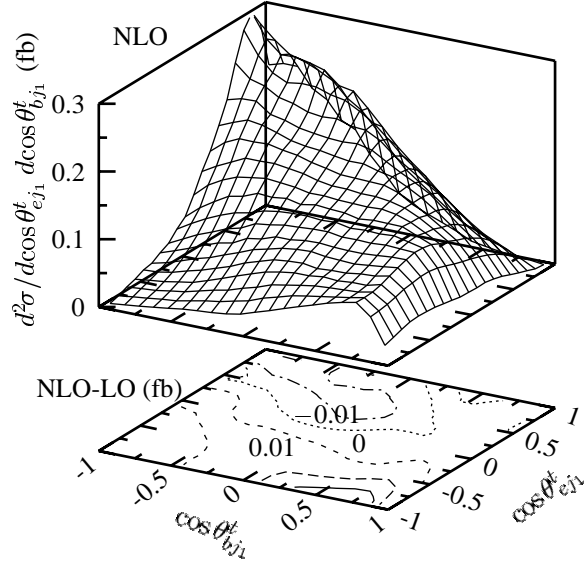


FIG. 12: Correlated angular distributions of the final-state particles in the top-quark rest frame of t -channel single-top-quark production at NLO (top), and the difference between NLO and LO (bottom). This is a two-dimensional projection between $\cos \theta_{ej_1}^t$, where e is the charged lepton and j_1 is tagged as the highest- E_T light-quark jet, and $\cos \theta_{bj_1}^t$, where b is the b jet from the top-quark decay.

t -channel and s -channel production as most of the events are piled up at small $\cos \theta_{eb}^t$ and large $\cos \theta_{ej_1}^t$. A slightly better cut would follow the contours of the peak, but this depends on the Wjj background that we show in Figs. 18–20. The first thing to notice is that our apparent shaping of the background actually was an artifact of removing one peak in the correlated distribution. Given the symmetry of the jets, the initial flat background for the $\cos \theta_{ej_1}^t$ distribution was due to the sum over two peaks in the full phase space with broad tails that accidentally compensated each other.

Based on the correlated distributions for the signal and background presented in Figs. 12–20, I propose the following series of acceptance cuts as a starting point to better isolate single-top-quark production:

1. $\cos \theta_{eb}^t < \cos \theta_{ej_1}^t$.
2. $\cos \theta_{bj_1}^t < \cos \theta_{ej_1}^t$.
3. $\cos \theta_{bj_1}^t < 0.6\text{--}0.8$.

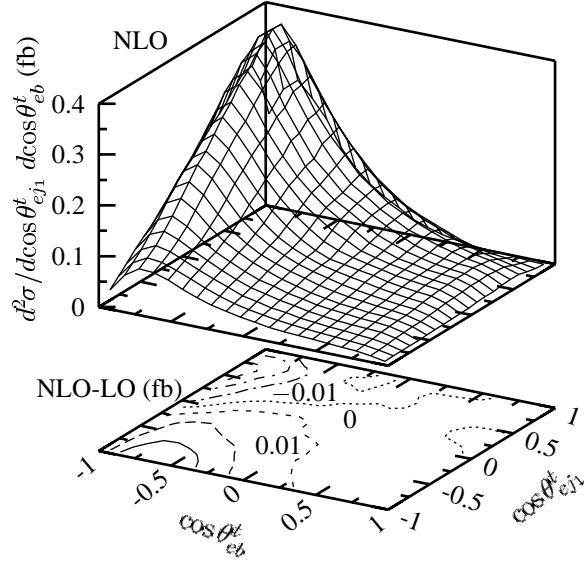


FIG. 13: Correlated angular distributions of the final-state particles in the top-quark rest frame of t -channel single-top-quark production at NLO (top), and the difference between NLO and LO (bottom). Same as Fig. 12, but projecting on $\cos \theta_{ej_1}^t$ and $\cos \theta_{eb}^t$.

$$4. \cos \theta_{ej_1}^t > 0-0.4 \text{ or } \cos \theta_{eb}^t > -0.8.$$

These cuts should be optimized based on full detector simulations, and replaced by more sophisticated parameterizations of the correlated space. We saw in Sec. II, and the t -channel plots⁴ above, that a leading-order matrix is good enough to represent the NLO correlations. Therefore, feeding the correlated matrix elements into a showering Monte Carlo like PYTHIA [15] or HERWIG [16] should allow for accurate modeling of the acceptances.

The s -channel production mode can make use of one strong additional acceptance cut. Most of the signal is contained in the box defined by $\cos \theta_{e\bar{p}}^t > -0.2$ and $\cos \theta_{ej_1}^t > 0.1$, as seen in Fig. 21. The Wjj backgrounds in Fig. 22, however, are nearly flat in both of these variables, except at the edges of phase space where jet cuts come in. While I do not include this cut in the numerical results below, up to 3/4 of the background may be removed for a small loss in signal if this cut is layered on top of the cuts listed above.

⁴ Differences between NLO and LO times a K factor in s -channel and Wjj correlated distributions are too small to reliably calculate, but are typically much less than 5%.

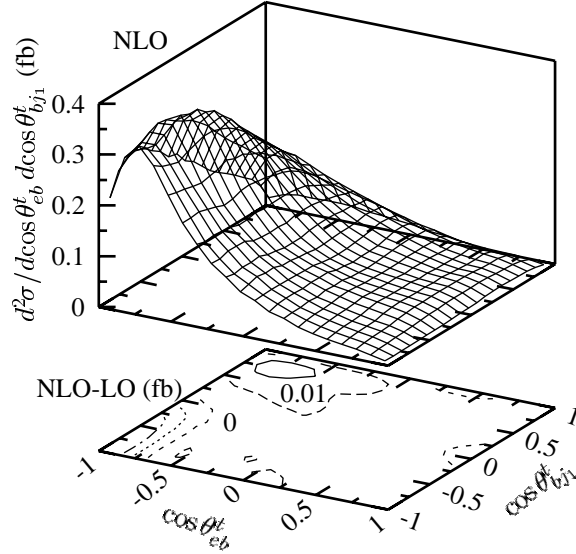


FIG. 14: Correlated angular distributions of the final-state particles in the top-quark rest frame of t -channel single-top-quark production at NLO (top), and the difference between NLO and LO (bottom). Same as Fig. 12, but projecting on $\cos \theta_{eb}^t$ and $\cos \theta_{bj_1}^t$.

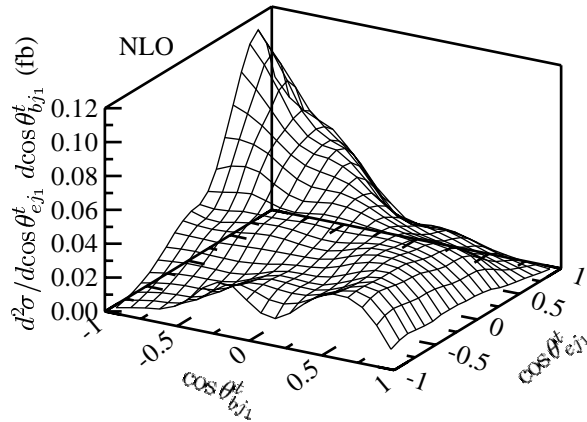


FIG. 15: Correlated angular distributions of the final-state particles in the top-quark rest frame of s -channel single-top-quark production at NLO. Labels are the same as in Fig. 12.

B. An additional discriminate

Now that fully differential NLO spin-dependent calculations are available, we can look for other correlations to separate signals and backgrounds. Subtle effects, such as how to define the neutrino in W reconstruction can have a sizable impact on measured cross sections. One of the other limiting issues in applying a top-quark mass cut is exactly how well the missing

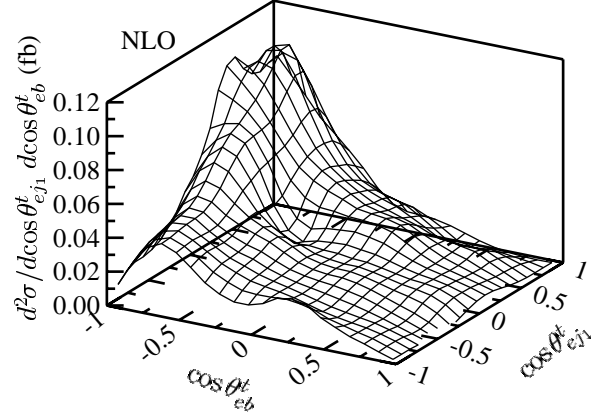


FIG. 16: Correlated angular distributions of the final-state particles in the top-quark rest frame of s -channel single-top-quark production at NLO. Same as Fig. 15, but projecting on $\cos \theta_{ej_1}^t$ and $\cos \theta_{eb}^t$.

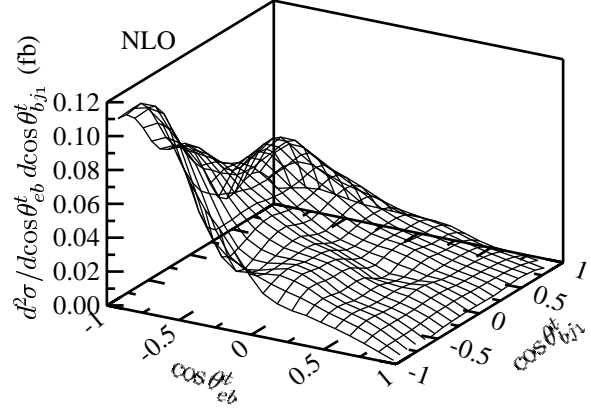


FIG. 17: Correlated angular distributions of the final-state particles in the top-quark rest frame of s -channel single-top-quark production at NLO. Same as Fig. 15, but projecting on $\cos \theta_{eb}^t$ and $\cos \theta_{bj_1}^t$.

energy can be measured, and fed into the top-quark reconstruction. To attempt to avoid this problem, I have also looked at the fully correlated combinations of invariant masses M_{ij} at NLO after cuts.

Most of the multi-dimensional correlated M_{ij} plots are similar between the single-top-quark signals and the Wjj backgrounds. Specifically, the tails of the distributions are almost identical, and the peak for signal is under a strongly rising background. Some cuts may help, but it is difficult to retain enough signal. The one exception is the projection along M_{bj_1} , as

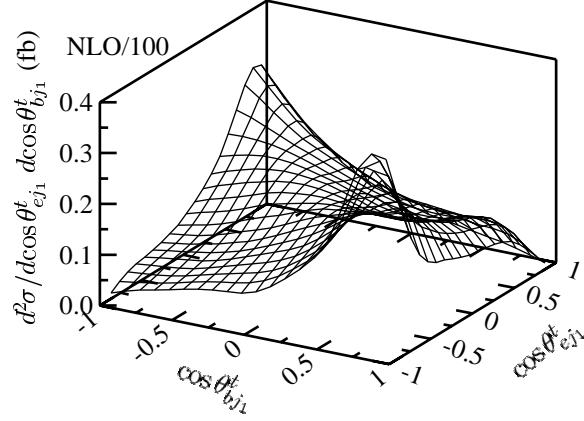


FIG. 18: Correlated angular distributions of the final-state particles in the reconstructed top-quark rest frame of Wjj production at NLO. Labels are the same as in Fig. 12.

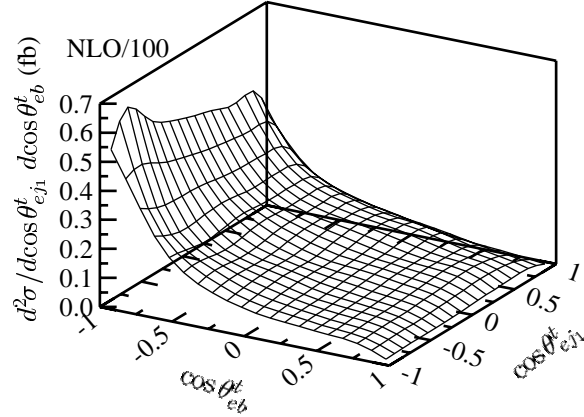


FIG. 19: Correlated angular distributions of the final-state particles in the reconstructed top-quark rest frame of Wjj production at NLO. Same as Fig. 18, but projecting on $\cos \theta_{ej_1}^t$ and $\cos \theta_{eb}^t$.

shown in Fig. 23. Applying a cut of $M_{bj_1} > 50\text{--}120$ GeV can reduce the background whether or not the top-quark mass can be reconstructed. We could have also raised the cut on E_{Tb} to 40 or 50 GeV, but the invariant mass is somewhat more selective.

IV. CONCLUSIONS

Cuts are virtually always made on angular distributions. Some of these cuts, like rejecting back-to-back jets to reduce mismeasurements, are difficult to avoid. Others enter indirectly from kinematically-dependent efficiencies, or reconstruction cuts, like fitting the top-quark

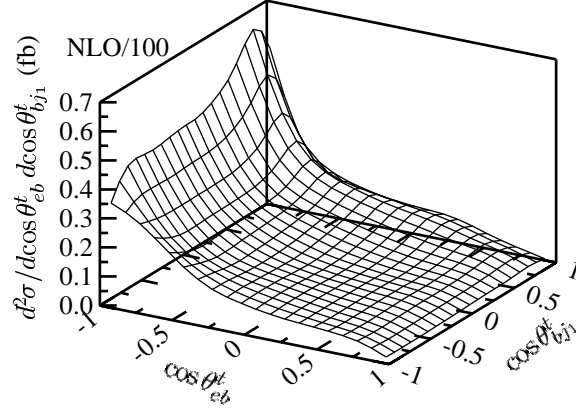


FIG. 20: Correlated angular distributions of the final-state particles in the reconstructed top-quark rest frame of Wjj production at NLO. Same as Fig. 18, but projecting on $\cos \theta_{eb}^t$ and $\cos \theta_{bj_1}^t$.

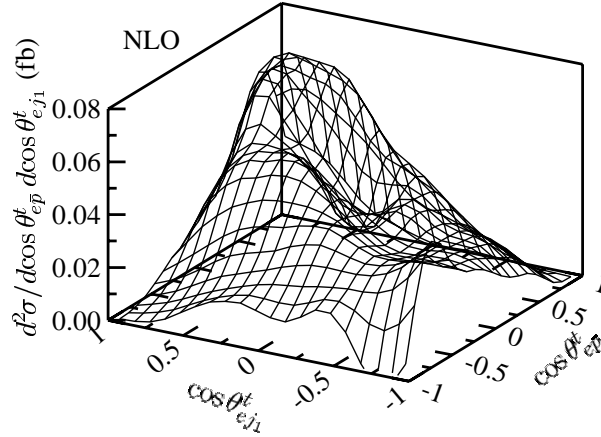


FIG. 21: Correlated angular distributions of the final-state particles in the top-quark rest frame of s -channel single-top-quark production at NLO. Same as Fig. 15, but projecting on $\cos \theta_{e\bar{p}}^t$ and $\cos \theta_{e j_1}^t$, where \bar{p} is the incoming antiproton.

mass. These cuts generically cause initially uncorrelated distributions, like $\cos \theta_{e j_1}^t$ for Wjj , to appear to fake our signals. By using more of the measured angles in the event, these artificially induced correlations can be reduced or removed. This will become even more vital at the LHC, where Standard Model backgrounds to new physics are large. To use this information reliably, however, will require studies that confirm that the predictions of the angular distributions are stable against higher-order radiation.

We have examined the relationship between the leading-order and next-to-leading order predictions of angular correlations of leptons and jets in the single-top-quark and Wjj final

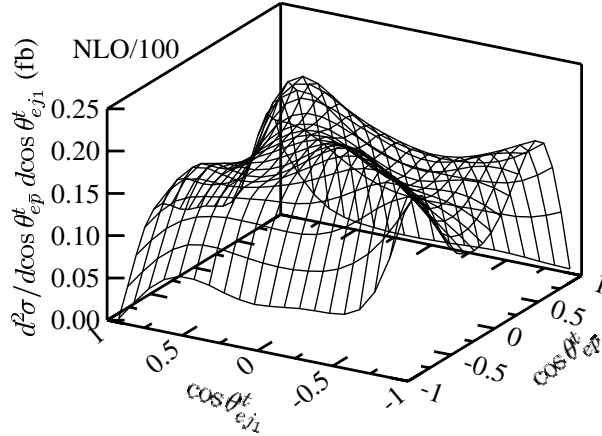


FIG. 22: Correlated angular distributions of the final-state particles in the reconstructed top-quark rest frame of Wjj production at NLO. Labels are the same as in Fig. 21.

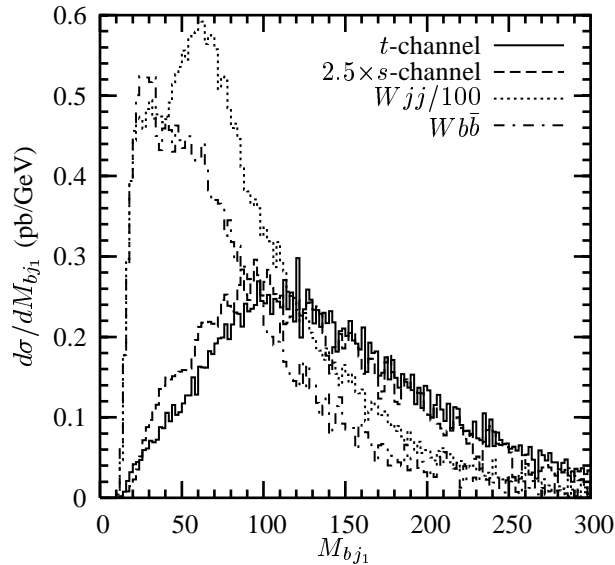


FIG. 23: Invariant mass of the identified b -jet and highest- E_T jet j_1 from t - and s -channel single-top-quark, Wjj , and $Wb\bar{b}$ production.

states. The good news is that LO matrix elements are sufficient to capture the complete angular correlations. The uncertainties induced by using LO matrix elements are less than 5% of the total acceptance in all cases. Hence, showering Monte Carlo generators that are fed with the spin-dependent matrix elements may be used to reliably construct an experimental analysis. The only place to be careful is in t -channel production, where matrix elements matched to NLO predictions are required to obtain the correct kinematics [10]. These

matched samples are already available and in use by both the CDF and D0 Collaborations.

This paper does not attempt to perform a fully simulated signal and background study. Nevertheless, if we apply the four angular cuts listed in Sec. III A, we can estimate that the significance only improves slightly, but the signal to background ratio S/B improves by a factor of 1.5. Adding the invariant-mass cut of Sec. III B improves the significance by roughly 25%, but, more importantly, improves S/B by almost a factor of 3. The complete set of cuts retains about 40% of the signal, but reduce the Wjj background by a factor of 7. These results should be further optimized after full detector simulations, but already represent the power inherent in using well-predicted angular correlations.

Acknowledgments

Research at Fermi National Accelerator Laboratory was supported by the U. S. Department of Energy, High Energy Physics Division, under contract No. DE-AC02-76CH03000. Research in the High Energy Physics Division at Argonne National Laboratory was supported by an FY2005 grant from the Argonne Theory Institute, and by the U. S. Department of Energy under Contract No. W-31-109-ENG-38.

-
- [1] CDF Collaboration, C. I. Ciobanu, *Int. J. Mod. Phys. A* **16S1A**, 389 (2001); CDF Collaboration, D. Acosta *et al.*, *Phys. Rev. D* **65**, 091102 (2002); CDF Collaboration, T. Kikuchi, S. K. Wolinski, L. Demortier, S. Kim, and P. Savard, *Int. J. Mod. Phys. A* **16S1A**, 382 (2001); CDF Collaboration, D. Acosta *et al.*, *Phys. Rev. D* **69**, 052003 (2004).
 - [2] D0 Collaboration, V. M. Abazov *et al.*, *Phys. Lett. B* **517**, 282 (2001); D0 Collaboration, B. Abbott *et al.*, *Phys. Rev. D* **63**, 031101 (2001); D0 Collaboration, A. P. Heinson, *Int. J. Mod. Phys. A* **16S1A**, 386 (2001).
 - [3] CDF Collaboration, D. Acosta *et al.*, *Phys. Rev. D* **71**, 012005 (2005).
 - [4] D0 Collaboration, V. Abazov *et al.*, *Phys. Lett. B* **622**, 265 (2005).
 - [5] M. T. Bowen, S. D. Ellis, and M. J. Strassler, *Acta Phys. Polon. B* **36**, 271 (2005).
 - [6] Q. H. Cao, R. Schwienhorst, and C. P. Yuan, *Phys. Rev. D* **71**, 054023 (2005); Q. H. Cao, R. Schwienhorst, J. A. Benitez, R. Brock, and C. P. Yuan, hep-ph/0504230.

- [7] T. Stelzer, Z. Sullivan, and S. Willenbrock, Phys. Rev. D **58**, 094021 (1998).
- [8] G. Mahlon and S. Parke, Phys. Rev. D **55**, 7249 (1997); Phys. Lett. B **476**, 323 (2000).
- [9] J. M. Campbell and R. K. Ellis, Phys. Rev. D **62**, 114012 (2000); Phys. Rev. D **65**, 113007 (2002); J. Campbell, R. K. Ellis, and F. Tramontano, Phys. Rev. D **70**, 094012 (2004).
- [10] Z. Sullivan, Phys. Rev. D **70**, 114012 (2004).
- [11] J. Pumplin, D. R. Stump, J. Huston, H. L. Lai, P. Nadolsky, and W. K. Tung, J. High Energy Phys. **07**, 012 (2002).
- [12] D. Stump, J. Huston, J. Pumplin, W. K. Tung, H. L. Lai, S. Kuhlmann, and J. F. Owens, J. High Energy Phys. **10**, 046 (2003).
- [13] B. W. Harris, E. Laenen, L. Phaf, Z. Sullivan, and S. Weinzierl, Phys. Rev. D **66**, 054024 (2002).
- [14] ATLAS Collaboration, D. O'Neil *et al.*, J. Phys. G **28**, 2657 (2002).
- [15] T. Sjöstrand *et al.*, Comput. Phys. Commun. **135**, 238 (2001).
- [16] G. Corcella *et al.*, J. High Energy Phys. **01**, 010 (2001).